We are IntechOpen, the world's leading publisher of Open Access books
Built by scientists, for scientists

4,800
Open access books available

122,000
International authors and editors

135M
Downloads

154
Countries delivered to

Our authors are among the

TOP 1%
most cited scientists

12.2%
Contributors from top 500 universities

BOOK CITATION INDEX
CLARIVATE ANALYTICS
INDEXED

WEB OF SCIENCE™

Selection of our books indexed in the Book Citation Index
in Web of Science™ Core Collection (BKCI)

Interested in publishing with us?
Contact book.department@intechopen.com

Numbers displayed above are based on latest data collected.
For more information visit www.intechopen.com

Characterization of Rice Husk Biofibre-Reinforced Recycled Thermoplastic Blend Biocomposite

Ruey Shan Chen and Sahrim Ahmad

Additional information is available at the end of the chapter

Abstract

In this century, the developing country has a high potential towards the growth of green composites, and therefore there is significant achievement in green technology especially in the field of building constructions and automotive because of the environment and sustainability issues. The market for development of advanced biocomposite materials produced from biomass and recyclable post-consumer plastics is increasing. Natural fibre-reinforced biocomposites based on rice husk biofibre (RHB), recycled high-density polyethylene (rHDPE) and recycled polyethylene terephthalate (rPET) were prepared through a two-step extrusion and hot pressing. The influence of thermoplastic blend (TPB) matrix types (uncompatibilized and compatibilized with 5 parts per hundred compound (phc) ethylene-glycidyl methacrylate (E-GMA) copolymer) and high fibre contents of 50, 60, 70 and 80 wt% RHB on the composite properties was studied. Maleic anhydride polyethylene (MAPE) was added as a coupling agent to enhance the interfacial adhesion of the fibre-matrix phases. Results showed that water absorption, thickness swelling (TS) and tensile and flexural properties enhanced tremendously with the increase of rice husk filler loadings. Biocomposites based on compatibilized blend matrix exhibited higher mechanical properties and dimensional stability than those based on uncompatibilized ones. Thermal analysis results from thermogravimetric analysis (TGA) and differential scanning calorimetry (DSC) indicated the notable improvement in thermal stability as the added rice husk (RH) fibre content increased. From these results, we can conclude that RHF can work well with rHDPE/rPET thermoplastic blend for manufacturing high loading biocomposite products.

Keywords: green composite, high fibre loading, recycled polymer blend, agro waste, melt blending, properties

1. Introduction

Nowadays, environmental friendliness is becoming one of the important criterions to be considered in material selection for the introduction of new materials and products resulting from global ecological concern and new rules and regulations [1, 2]. Waste plastic industrial and agricultural materials are currently becoming of interest worldwide in the field of composite materials, as a result of the increasing demand for environmentally friendly raw materials. The development of new biocomposites composed of recycled materials by post-consumer polymers as matrixes and agro-waste fibres as reinforcement phases and the better understanding of their fibre-matrix interactions will enhance their aggregated values and applications. Consequently, these reduce their environmental impact as waste materials and help to close the carbon cycle and manufacture greener composites [3, 4]. Natural fibre-reinforced thermoplastic composites have been used in various applications as furniture and architectural materials and, more recently, in the construction and automotive industry [5, 6].

Malaysia is well endowed with rich and renewable natural tropical forest resources which provide a variety of natural fibres. Rice husk (RH), one type of natural fibres, is an agricultural industrial residue generated during the rice-milling process in rice-producing countries, especially in the Asian, Pacific and North American regions [7]. In the paddy plants of Malaysia, with a land area of approximately 680 thousand hectares, a total of 840 thousand tons of RH is produced annually [8]. For every one million tonnes of paddy rice harvested, it is estimated that about 200 thousand tonnes of the RH was used for the purposes as fuel sources, animal beddings and landfill. The raw RH comprises several components with different percentages that are 25–35 % of cellulose, 18–21 % of hemicellulose, 26–31 % of lignin, 15–17 % of silica, 2–5 % of solubles and 7.5 % of moisture content. The use of RH in composite industry might be because of its low cost and bulk density, abundant, toughness, abrasive in nature, resistance to weathering, renewability, biodegradability and nonhazardousness [9, 10]. Compared to wood-based composites, the composites containing RH possess better water absorption and dimensional stability, as well as higher resistance to biological and termite attack. Therefore, these composites are progressively being used in automotive industry for interior parts such as car trims and door panels and in the building construction like interior panels, decks and window and door frames [7].

The worldwide fabrication and consumption of plastics have resulted in a remarkable contribution to municipal solid waste (MSW) [11]. For example, plastic wastes accounts for 24 % of the annual 7.7 million tonnes of the MSW generated in Peninsular Malaysia with the population of 28.45 million inhabitations in 2010 [12]. Majority of them consist of a significant amount of polyethylene (PE) and polyethylene terephthalate (PET) [13]. High-density poly-ethylene (HDPE) and PET are widely used in packaging industry, and their annual rates of consumption are kept increasing. Blends of HDPE/PET possess the intermediate characteristics and properties between both polymer components. As compared to PET, they have lower brittleness; as compared to HDPE, they have higher stiffness, flow better and are fast cooling. It has been revealed that ethylene-glycidyl methacrylate (E-GMA) copolymer serves as the most effective compatibilizer in order to enhance the miscibility between the hydrophobic

HDPE and hydrophilic PET, thus improving the blend properties [14]. The resultant blends made of recycled polymers have been used in wood-plastic composites (WPC) as matrices [15].

Both thermoplastic and thermoset polymers either in the form of virgin or recycled can be used in the manufacture of natural fibre-polymer composites (NFPCs). Because recycled polymers are produced in large amounts daily and are cheaper than virgin polymers, the waste polymers offer a promising raw material source for the composites [16]. Traditionally, a single type of polymer is used as matrix in NFPCs [16–18]. However, there are very limited studies on the NFPCs made of polymer blends [15, 19].

In this chapter, the influence of rice husk biofibre (RHB) contents (50–80 wt%) on the physical, mechanical, thermal and morphological properties of recycled thermoplastic blend (TPB) was investigated.

2. Experimental details

Thermoplastic blend (TPB) matrix used recycled high-density polyethylene (rHDPE) with a density of 923 kg/m^3 and melt flow index of 0.72 g/10 min at 190 °C and recycled polyethylene terephthalate (rPET) with an intrinsic viscosity of 0.68 dL/g. Ethylene-glycidyl methacrylate (E-GMA) copolymer (trade name of Lotader AX8840), with a melt flow index of 5 g/10 min at 190 °C and a glycidyl methacrylate content of 8 %, was used as compatibilizer for immiscible TPB. Rice husk flour (RHF) with particle size of 100 mesh was used as agro-waste filler. Maleic anhydride polyethylene (MAPE), a coupling agent with a melting peak temperature of 135.2 °C, was used. All the raw materials were supplied by a local factory, namely, Bio Composite Extrusions Sdn. Bhd.

2.1. Preparation of thermoplastic blend (TPB)

The rHDPE and rPET were compounded via extrusion process by using a laboratory-scale co-rotating twin screw extruder (Thermo Prism TSE 16 PC). The screw-rotating speed was fixed at 30 rpm. The four barrel temperatures from feeding to die zones were set as 250, 270, 240 and 190 °C, respectively. For the uncompatibilized thermoplastic blend (UTPB), the weight ratio of rHDPE/rPET was fixed at 75/25 (wt%). Meanwhile, 5 parts per hundred compounds (phc) of E-GMA was added in the compatibilized thermoplastic blend (CTPB) with the same ratio of both plastics.

2.2. Preparation of RHF-reinforced biocomposites

The pre-extruded TPB pellets were compounded with RHF and 3 phc of MAPE at temperature profiles of 170, 215, 210 and 195 °C and screw speed of 30 rpm. Prior to extrusion, RHF was oven-dried at 90 °C for 24 h to remove the moisture of RHF. After extrusion, the compression moulding was performed at 200 °C using a hot/cold press machine (LP50, Labtech Engineering Company Ltd.). The preheating, venting, full pressing and cold pressing times were set at 3,

2, 5 and 5 min, respectively. In this study, the experimental variables studied were polymer blend types (UTPB and CTPB) and rice husk flour content (50, 60, 70 and 80 wt%).

2.3. Characterization

Water absorption and thickness swelling (TS) tests were performed according to the ASTM D 570-98 method. The specimen (dimension: 76.2 × 25.4 × 3.2 mm) for each formulation was oven-dried for 24 h at 100 °C. Each oven-dried specimen was weighed using an analytical balance with a precision of 1 mg; the thickness of each oven-dried specimen was measured using a digital calliper with a precision of 0.01 mm. The specimens were then soaked in distilled water at 25 °C. The weight and thickness changes were determined periodically until 119 days. Specimens were removed from the water, wiped dry with tissue paper and measured. The percentages of water absorption (WA) and thickness swelling (TS) were calculated using Eqs. 1 and 2:

$$WA\ (\%) = \frac{W_t - W_0}{W_0} \times 100 \tag{1}$$

$$TS(\%) = \frac{T_t - T_0}{T_0} \times 100 \tag{2}$$

where W_0 and W_t represent the oven-dry weight (the initial weight) and weight after water exposure at time t, respectively, whereas T_0 and T_t represent the oven-dry thickness and thickness after water exposure at time t, respectively. Three replicates of specimens were tested for each formulation to obtain the average results.

Compression-moulded composite panels were cut according to ASTM D 638-03 (type I) for tensile testing, ASTM D 790-03 for flexural testing and ASTM D 256-05 for impact strength. Both tensile and flexural testings are carried out using a universal testing machine (model Testometric M350-10CT) at 5 mm/min. The notched Izod impact testing was performed using the Ray-Ran Universal Pendulum Impact System at 3.46 ms^{-1} and 2.765 J with a load weight of 0.452 kg. In mechanical tests, five replicates of specimens were tested for each formulation to obtain the average results.

Thermogravimetric analysis (TGA) and differential scanning calorimetry (DSC) were conducted using a Mettler Toledo TGA/SDTA851e and DSC 882e, respectively, on the samples of about 10–15 mg. Samples of TGA were tested at a heating rate of 10 °C/min over the temperature range from 25 °C to 600 °C, the temperature of complete degradation. Balance accuracy of TGA is ± 0.1 %. The DSC samples were scanned from 25 °C to 300 °C at heating rate of 10 °C/min, under atmospheric air flow condition. Burning test was carried out in accordance to ASTM D 5048-90 (procedure A—test of bar specimens) to determine the relative burning characteristics and flame-resistance properties. The burning rates of specimens are calculated using the

equation of $V = L/t$ where V is the burning rates (mm/s), L is the burned length (mm) and t is the burning time (seconds).

The morphology of the fracture surface of broken sample from tensile testing was analysed using SEM (VPSEM Philips XL-30). The samples were sputter-coated with gold before examination of SEM.

3. Results and discussion

3.1. Long-term water absorption and thickness swelling

Theoretically, the shape of the sorption curve plotted with experimental values is represented by the Fick's equation as $\log(M_t/M_m) = \log(k) + n\log(t)$, where M_t is the water absorbed at time t, M_m is the maximum water absorbed at saturation point and k and n are the diffusion kinetic parameters. The n values determined the diffusion behaviour cases: case I ($n = 0.5$) is Fickian diffusion, case II ($n \geq 1$) is relaxation controlled, and case III ($0.5 < n < 1$). The k values represent the interaction between the material and moisture. Both coefficients of n and k are determined from the slope and intercept of log plot of M_t/M_m versus t which can be drawn from experimental data, respectively [1]. As shown in **Table 1**, the value of n is close to 0.5 which confirmed that all the investigated biocomposites exhibited Fickian diffusion behaviour. The k value was found to increase with the increasing wt% of RHB in the biocomposites irrespective of the TPB matrix types, in which a higher value of k indicates that the biocomposite attained the saturation point of WA in a shorter period of time. This was due to the increased hydroxyl and carbonyl groups as the RHB content increased [2].

Composite samples	n	k (h^{-n})	M_m (%)	$D \times 10^{-13}$ (m^2 s^{-1})	TS_∞ (%)	$K_{SR} \times 10^{-3}$ (h^{-1})
Biocomposite UTPB/RHB						
0 wt% RHB	–	–	0.22 ± 0.04	–	0.19 ± 0.03	–
50 wt% RHB	0.467	0.021	8.76 ± 0.32	1.84 ± 0.09	4.94 ± 0.68	3.53 ± 0.17
60 wt% RHB	0.522	0.022	13.73 ± 0.55	3.47 ± 0.13	5.49 ± 0.75	4.39 ± 0.31
70 wt% RHB	0.511	0.025	14.16 ± 0.59	5.66 ± 0.49	6.76 ± 0.58	4.50 ± 0.43
80 wt% RHB	0.489	0.800	18.97 ± 0.73	42.54 ± 1.05	9.41 ± 0.77	10.29 ± 0.82
Biocomposite CTPB/RHB						
0 wt% RHB	–	–	0.14 ± 0.02	–	0.14 ± 0.01	–
50 wt% RHB	0.504	0.019	6.92 ± 0.22	2.02 ± 0.06	4.17 ± 0.26	2.10 ± 0.14
60 wt% RHB	0.470	0.020	9.96 ± 0.43	2.04 ± 0.11	4.56 ± 0.34	2.21 ± 0.16
70 wt% RHB	0.524	0.023	13.13 ± 0.67	5.35 ± 0.37	6.08 ± 0.52	3.74 ± 0.28
80 wt% RHB	0.496	0.028	14.71 ± 0.84	6.46 ± 0.61	8.71 ± 0.79	4.66 ± 0.50

Table 1. Diffusion kinetic parameters, coefficients and permeability of biocomposites.

The diffusion coefficient D represents the ability of water molecules to penetrate inside the composites, which can be computed with Eq. 3, in the case where the M_t value is < 60 % of the M_m value.

$$D = \pi \left[\frac{\theta}{4M_m} \right] \qquad (3)$$

where D is the diffusion coefficient, θ is the slope of the linear portion of M_t against $\sqrt{t}/h$ / and h is the height (thickness) of composite panel [3]. In **Table 1**, the M_m and D increase with the RHB content which indicates that the biocomposites containing the higher wt% of natural fibre tended to absorb more water. This phenomenon could be explained by the components of RHB (cellulose, hemicellulose and lignin) that mostly contain polar hydroxyl groups which tend to combine with water molecules by forming hydrogen bond [4]. The difference in D between UTPB and CTPB matrixes was more predominant in the biocomposites at higher wt% of fibre. Especially at 80 wt% RHB, a remarkable decrease in M_m and D was observed for the biocomposites based on CTPB matrix as compared to UTPB ones. This confirmed the reduction of water absorption. This was probably because the free hydroxyl and carboxyl groups available in hydrophilic rPET play the role in absorbing water as there are lack of chemical interaction and bonding between polar rPET and nonpolar rHDPE chains in the case of without compatibilizer in the UTPB matrix [5]. Meanwhile, the presence of E-GMA compatibilizer tended to bind the rHDPE and rPET together, hence decreasing the hydrophilicity of CTPB matrix as well as reducing the WA.

The theoretical WA can be estimated using Fick's second law of diffusion. For the initial part of the curve where $M_t/M_m < 0.6$ [6], it can be predicted using Eq. 4. For the second half-sorption curve where $M_t/M_m > 0.6$ [6], an approximation has been proposed with Eq. 5 [7]:

$$\frac{M_t}{M_m} = \frac{4}{h}\sqrt{\frac{D.t}{\pi}} \qquad (4)$$

$$\frac{M_t}{M_m} = 1 - \exp\left[-7.3 \left(\frac{D.t}{h^2} \right)^{0.75} \right] \qquad (5)$$

Figures 1 and **2** depict the long-term WA of TPB/RHB biocomposites measured after a certain period of immersion in distilled water, respectively. The experimental data, as represented by the various symbols, show that the water absorbed by the biocomposites increased sharply with time and then gradually slowed until it reached an equilibrium state (M_m). The solid curves display the estimation of theoretical WA behaviour following Fick's second law of diffusion (Eqs. 4 and 5). All the curves in both **Figures 1** and **2** were found to follow the Fickian-type behaviour, as conformed to the coefficient of n which was close to 0.5 (**Table 1**). Thus, it

can be concluded that the experimental results will fit the Fickian mode of diffusion, especially in the initial stage of diffusion. This result is in agreement with the previous studies on polymer/natural fibre composites [6, 8]. **Figures 3** and **4** present the thickness swelling (TS) of immersed UTPB and CTPB biocomposites filled with RHB. It can be observed that TS was positively related to the WA where TS increased rapidly in the initial stage for all RHB contents and then remained constant. The higher the RHB loading, the more hydrogen bonding was created in the fibre cell wall by the adsorbed water, and thus, the higher TS of biocomposites was obtained.
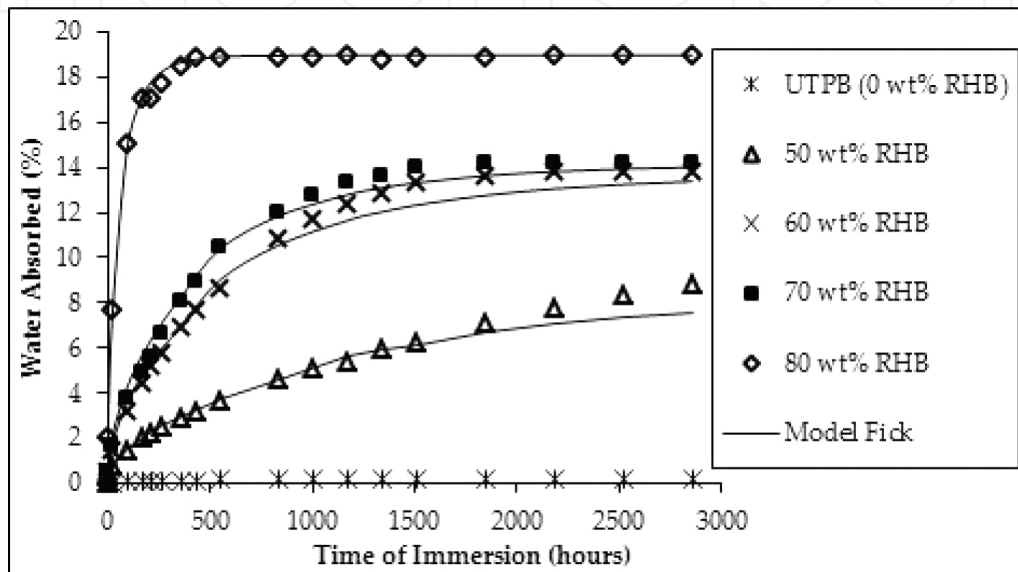
Figure 1. Water absorption of immersed UTPB/RHB biocomposites after a certain period.
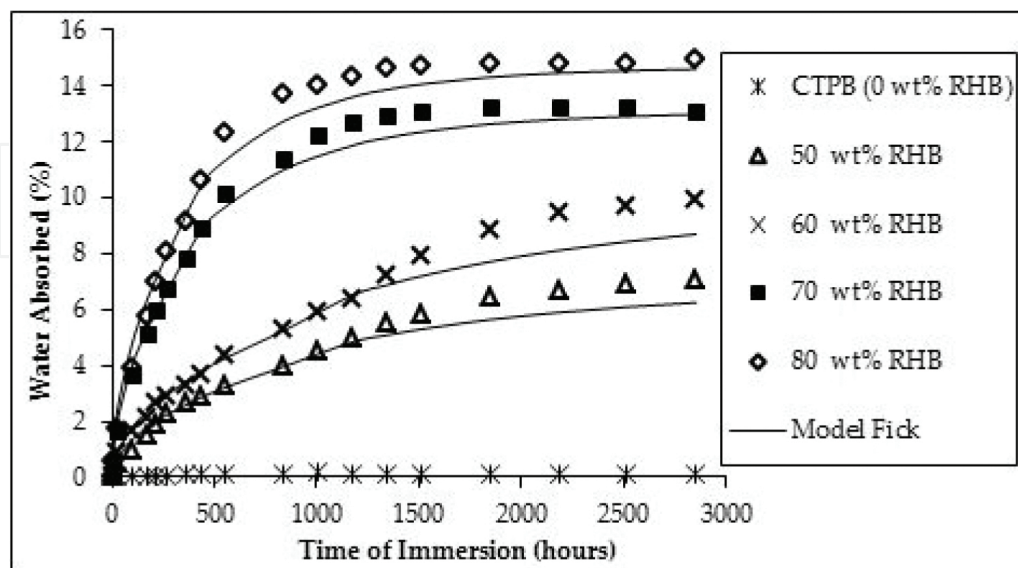
Figure 2. Water absorption of immersed CTPB/RHB biocomposites after a certain period.
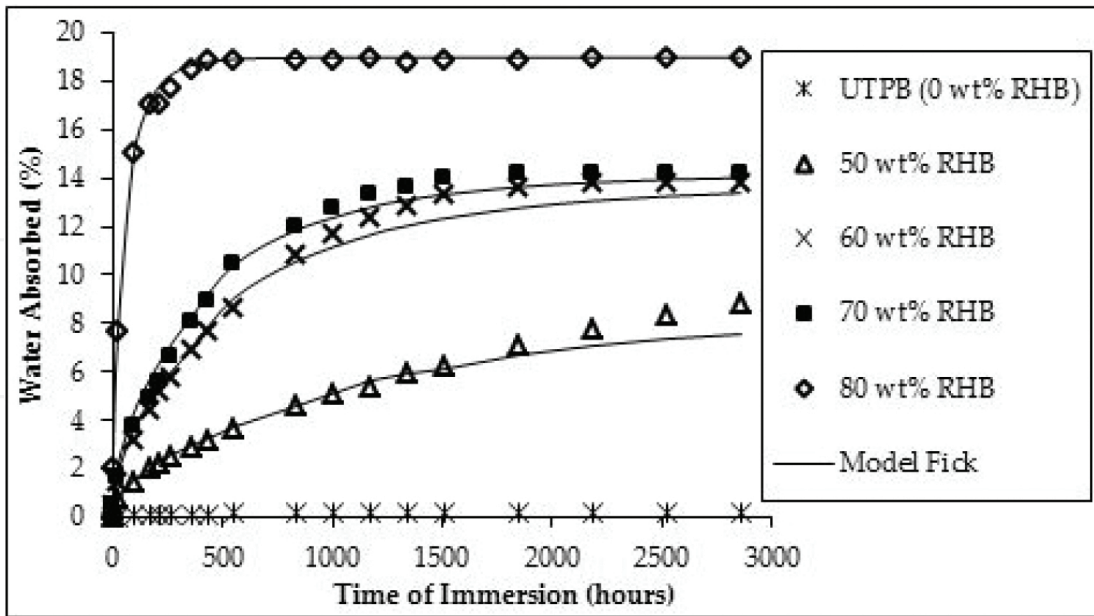
Figure 3. Thickness swelling of immersed UTPB/RHB biocomposites after a certain period.
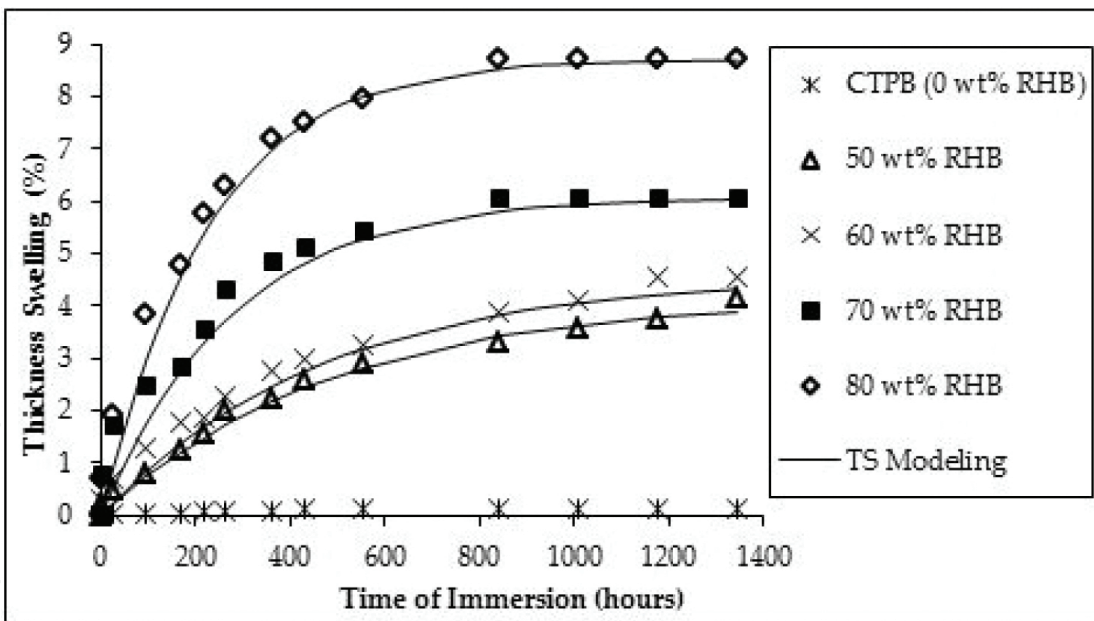

Figure 4. Thickness swelling of immersed CTPB/RHB biocomposites after a certain period.

Theoretically, the swelling behaviour can be computed by the model suggested by Shi and Gardner [9], which gives Eq. 6 after being rearranged and taking the natural logarithm:

$$\ln\left(\frac{100T_{\infty}}{\text{TS}(t)+100}-T_0\right)=\ln(T_{\infty}-T_0)-K_{SR}t \qquad (6)$$

where TS(t) is the TS at time t, T_∞ and T_0 are the equilibrium and initial thickness of sample, respectively, and K_{SR} is the intrinsic relative swelling rate (a constant). As shown in **Table 1**, the T_∞ and K_{SR} values increased with the RHB wt%, which indicates the higher swelling rate that the composite required a shorter time to reach the equilibrium TS [10]. The CTPB/RHB biocomposites exhibited lower K_{SR} values than that of UTPB/RHB biocomposites. This was probably attributed to better compatibility of TPB matrix which led to better fibre-matrix adhesion, and thus the water was difficult to access in the cellulose [2]. From **Figures 3** and **4**, the experimental results fitted well with the predicted TS from swelling model (solid curve).

3.2. Tensile properties

The influences of the TPB matrix types and RHB contents on the tensile strength and elastic modulus of biocomposites are presented in **Figures 5** and **6**, respectively. In general, the compatibilization of incompatible rHDPE and rPET by E-GMA was capable to improve the tensile properties of CTPB-based biocomposites with and without the presence of RHB. This was because of the E-GMA copolymer that acted as compatibilizer in order to enhance the compatibility and adhesion between rHDPE and rPET components [11]. Therefore, the CTPB blend and composites possessed higher tensile strength and elastic modulus than the UTPB ones.
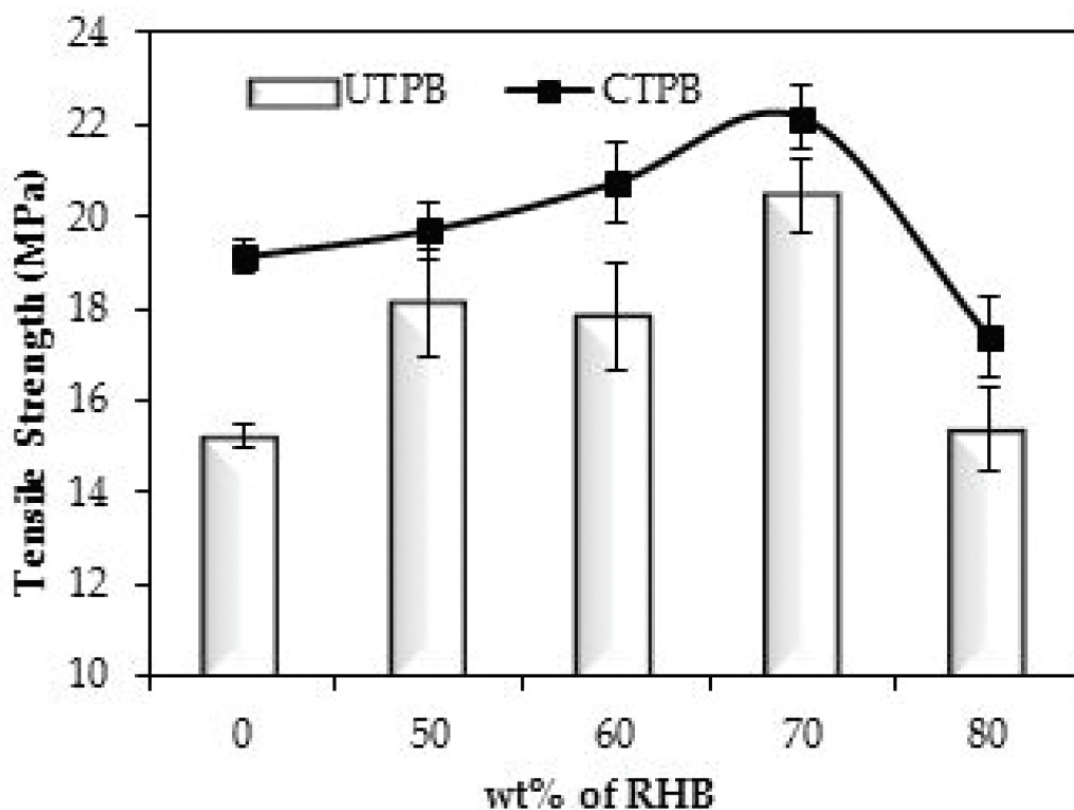

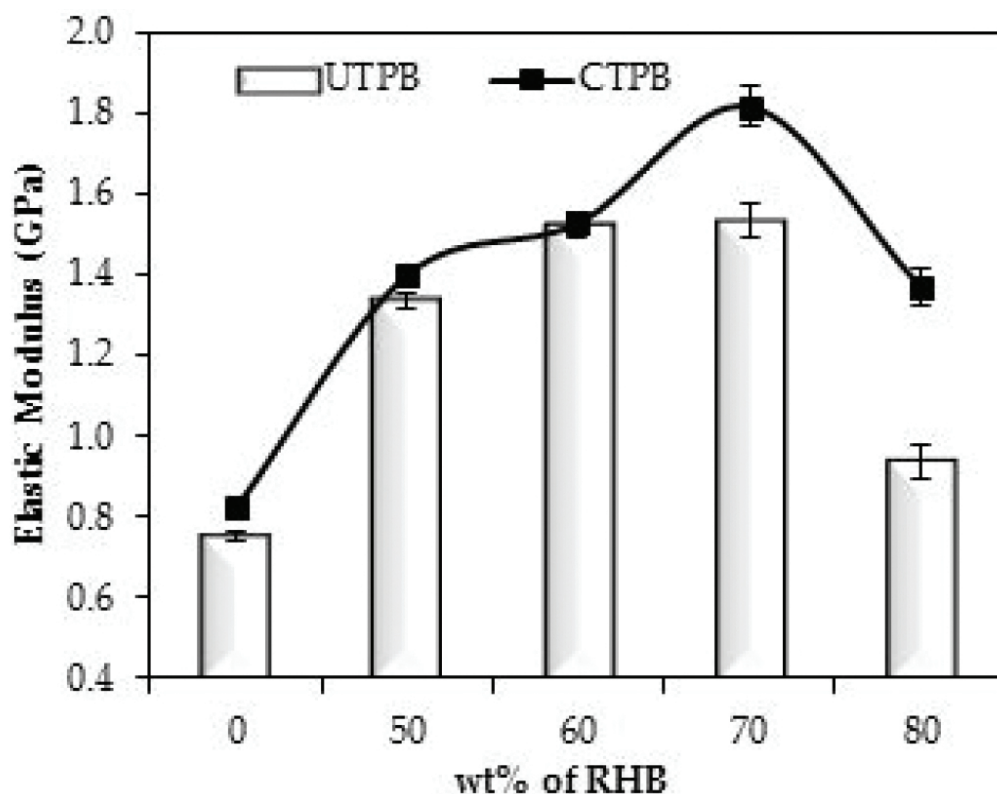**Figure 5.** Tensile strength of TPB/RHB biocomposites.

Figure 6. Elastic modulus of TPB/RHB biocomposites.

From **Figure 5**, both composites based on UTPB and CTPB show a similar trend. Tensile strength increased with increasing RHB up to maximum values achieved at 70 wt%, which were 20.5 and 22.2 MPa, respectively, for UTPB- and CTPB-based composites. This phenomenon suggests that the adhesion and interfacial bonding between the hydrophilic fibre and hydrophobic matrix are enhanced via the surface modification by coupling agent (MAPE) in which RHB can effectively transfer stress to each other [12]. As RHB content increased up to 80 wt%, it is found that tensile strength of composite decreased but the values were still higher than the pure blend (UTPB and CTPB). This possible reason is that the fibres acted as defects when the content of RHB exceeded the limit, which was at 70 wt% in this study. At high fibre content, fibres were not sufficiently wetted by the matrix (lower content), and this resulted in the fibre agglomerations which blocked the stress distribution. This could be further explained by the fact that the high content of RHB will need higher amount of coupling agent in order to give better interfacial adhesion and reinforcement effect with polymer matrix [13]. Somehow, CTPB-based composites exhibited higher values of tensile strength than that of UTPB-based composites. On the other hand, the increase of elastic modulus (**Figure 6**) with the RHB content (0–70 wt%) can be related to the enhanced stiffness which was imparted by the intrinsic characteristic of RHB. This trend is logic for biocomposite containing low stiffness polymer matrix and high stiffness filler [12]. However, elastic modulus is reduced when 80 wt% RHB is added into the composite. This may be due to the weaker interfacial interaction of RHB-polymer matrix and rHDPE-rPET in UTPB matrix.

3.3. Flexural properties

Figures 7 and **8** depict the modulus of rupture (MOR) and modulus of elasticity (MOE) of biocomposites based on two types of TPB with different contents of RHB.
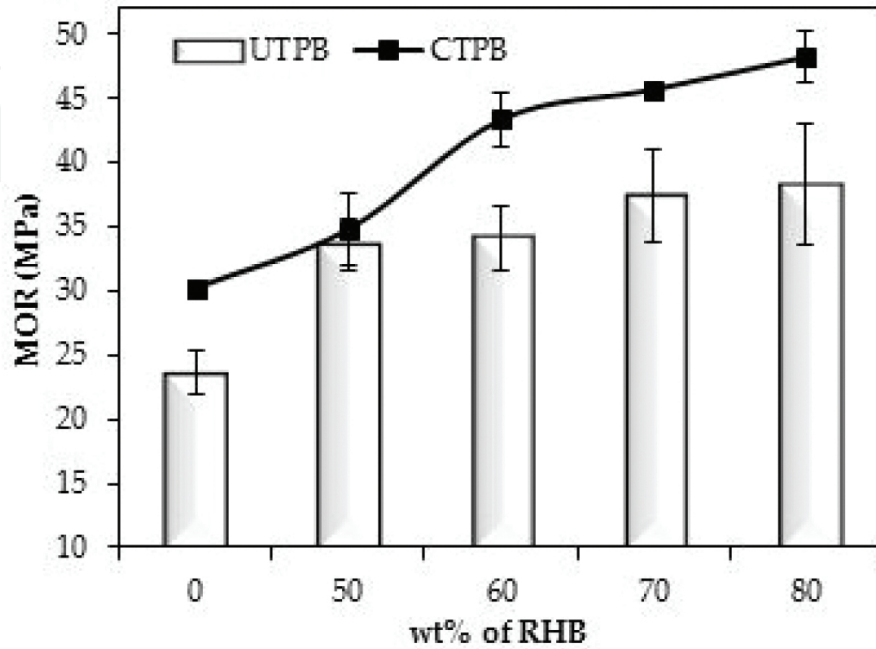

Figure 7. Modulus of rupture (MOR) of TPB/RHB biocomposites.
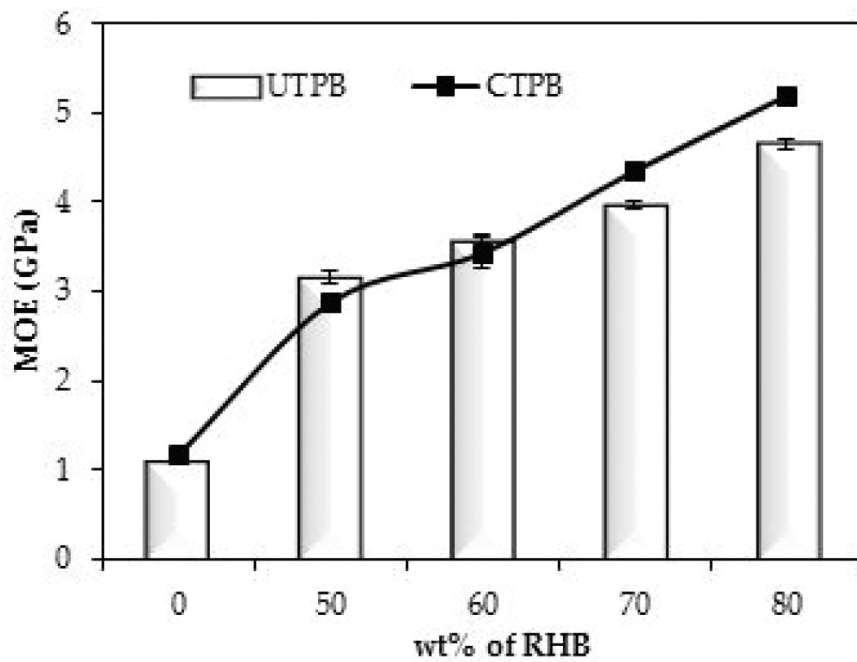

Figure 8. Modulus of elasticity (MOE) of TPB/RHB biocomposites.

The results showed that the presence of RHB improved the flexural properties of biocomposites. In **Figure 7**, CTPB-based biocomposites had higher MOR values than the UTPB-based biocomposites. This was attributed to the compatibilizing reaction for inherently immiscible TPB matrix which then improved adhesion between fibre and polymer blend matrix besides the enhanced compatibility between polymer blend components. Meanwhile, the incorporation of E-GMA into the CTPB matrix seemed not to provide a significant effect in the MOE of biocomposites (**Figure 8**). Comparing to UTPB-based composite, the MOE for CTPB-based composite reinforced with 50–60 wt% RHB was slightly lower. This phenomenon is associated to the weak intrinsic mechanical properties of E-GMA [14]. However, for the composites with higher content of RHB (70–80 wt%), this factor can be negligible due to relatively low content of the matrix (30 wt% and lower).

3.4. Impact properties

Figure 9 presents the impact strength of TPB/RHB biocomposites. For neat blends without the presence of RHB, compatibilization reaction of E-GMA provided a reinforcement effect and led to a significant increase of impact strength for CTPB matrix. However, this large improvement decreased when RHB was added to the blend matrix, which was because rice husk is one kind of stiff inorganic fillers [15]. The impact strength is reduced with RHB content. At high fibre content, there were many interactions between fillers as a result of the filler agglomerations in the composite which were more susceptible to the cracks than the fibre-matrix interface. This indicates that the cracks spread more easily in the biocomposites with high content of rice husk, thus decreasing the impact strength [16].
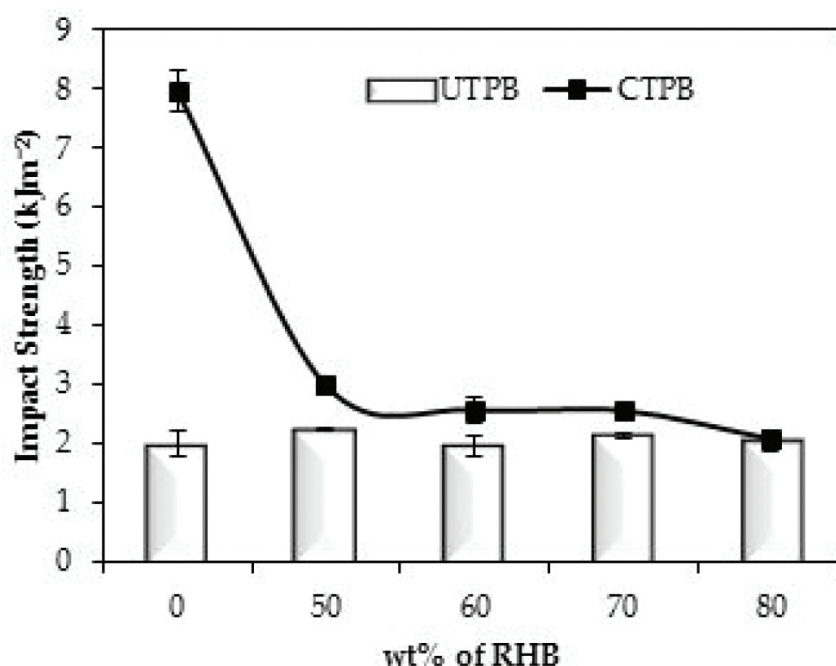

Figure 9. Impact strength of TPB/RHB biocomposites.

3.5. Differential scanning calorimetry (DSC)

Figure 10 depicts the melting temperature (T_m) of (a) rHDPE and (b) rPET components for TPB/RHB biocomposites that are measured from DSC testing. According to Kiziltas et al. (2011), the T_m of the composites plays a crucial role in determining the processing temperature and thermal properties [17]. As shown in **Figure 10**, neat UTPB showed a T_m of rHDPE component at 135.6 °C and T_m of rPET component at 252.8 °C, whereas neat CTPB possessed a lower T_m values of about 133.6 °C for rHDPE and 251.2 °C for rPET which were attributed to the improvement of compatibility between two polymer components with the use of E-GMA as compatibilizer. The reduced T_m values by the addition of E-GMA might be because E-GMA has lower molecular mass which promotes the composite degradation at lower temperature values. In overall, it can be observed that the addition of RHB into polymer blend reduced the T_m by approximately 1.2–5.2 °C. This phenomenon proved the enhancement in the processing temperature of rHDPE after reinforced with RHB [18].
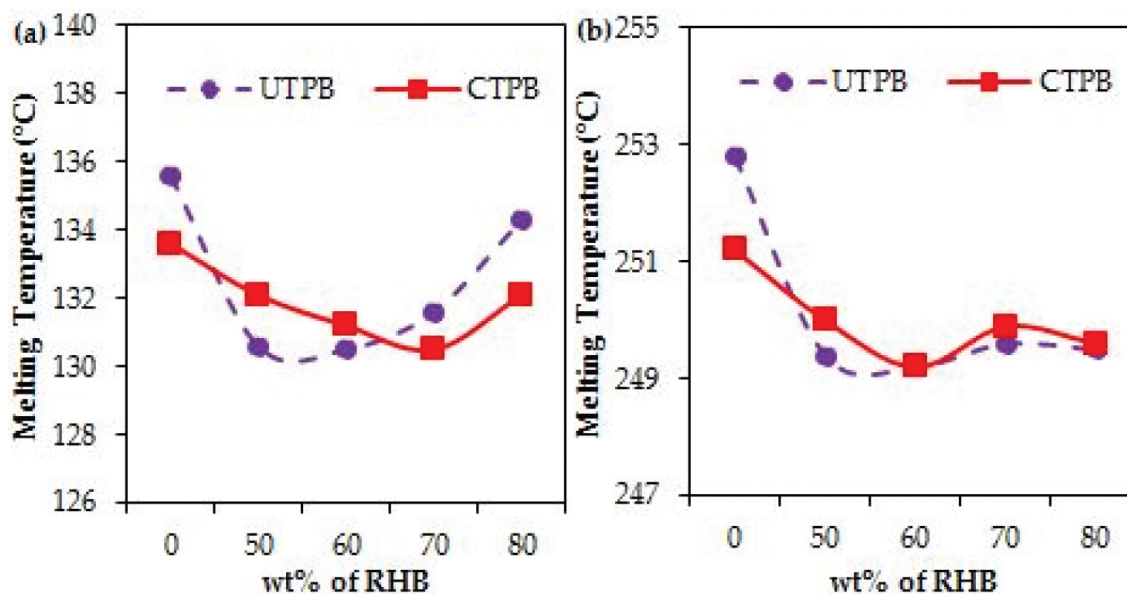

Figure 10. Melting temperature of (a) rHDPE and (b) rPET components in biocomposites.

Besides T_m, DSC testing also has provided the data of crystallinity level (χ_c) for TPB/RHB biocomposites, as presented in **Figure 11**. It was noted that the increasing RHB content from 50 to 80 wt% reduced the χ_c of TPB/RHB biocomposites. This was due to the incorporation of RHB that restricted the movement of polyethylene (PE) chain from crystallization process [19]. The CTPB/RHB biocomposites exhibited higher percentage of crystallinity than that of UTPB/RHB biocomposites. This suggests that the presence of E-GMA in the CTPB matrix improved the crystallinity by promoting the migration and diffusion of PE chains in order to form crystals in the surrounding of the rice husk surface. Several previous research results have reported that the addition of coupling agent copolymer enhanced the crystallinity of biocomposites [20, 21].
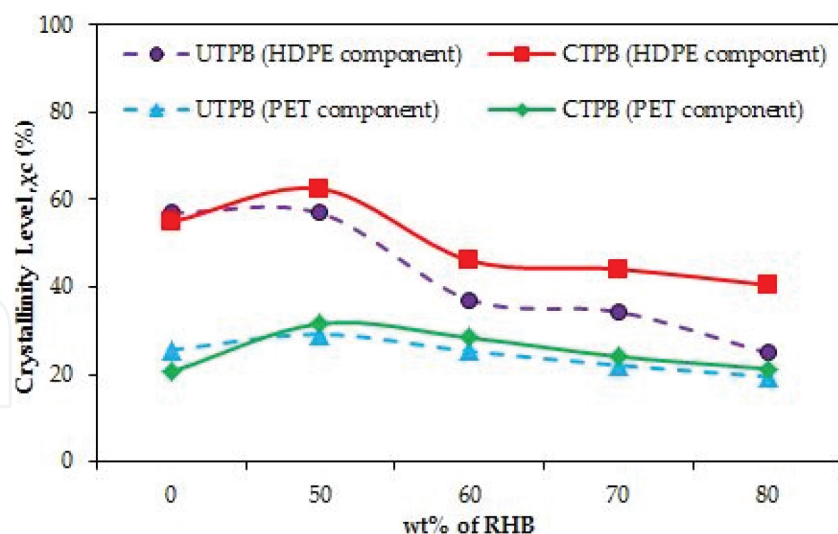
Figure 11. Crystallinity level (χ_c) of TPB/RHB biocomposites.

3.6. Thermogravimetric analysis (TGA)

Figure 12 presents (a) decomposition temperature (T_d) and (b) residues after heating at 600 °C that were obtained from TGA thermogram of TPB/RHB biocomposites. The neat UTPB and CTPB exhibited a one-step weight loss from 400 °C to 500 °C with the maximum decomposition temperature (T_d) at 471 °C and 469 °C, respectively (**Figure 12(a)**). This process occurred because the neat polymer blend comprised a series of interchained monomers, where an increase of temperature promoted the random chain scission through thermal degradation and depolymerization (at T_d) [22]. The lower T_d for CTPB than that of UTPB was due to an increase of rHDPE-rPET interaction because of the addition of E-GMA compatibilizer which possessed a lower decomposition temperature [23].
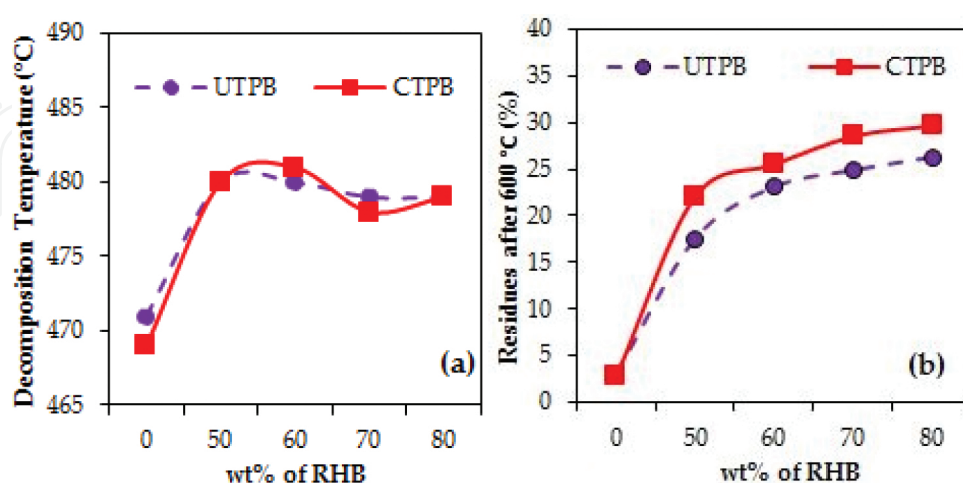

Figure 12. TGA thermogram data: (a) main decomposition temperature (T_d) of polymer component and (b) residues after 600 °C for TPB/RHB biocomposites.

In the presence of RHB in TPB matrix, the peaks of T_d have shifted to higher temperatures (478–481 °C), irrespective of matrix types and RHB contents. This behaviour suggests the improvement of thermal stability of TPB matrix by the incorporation of RHB that restricted the movement of polymer chains and thus delayed the thermal degradation process. Upon heating at temperature beyond 600 °C, both the neat UTPB and CTPB showed the relatively small amount of residues (**Figure 12(b)**). This is because the thermal degraded polymeric materials will further breakdown into gaseous products at higher heating temperature after T_d [22]. It can be observed that the residue weight of samples increased continuously with the increase of RHB content, up to 26.3 % and 29.6 % for composites containing 80 wt% RHB based on UTPB and CTPB matrix, respectively. These results were consistent with the high amount of silica present in the RHB.

3.7. Fire retardancy

Figure 13 shows the burning rate of both UTPB- and CTPB-based biocomposites filled with RHB. The neat TPB had the highest burning rate that was about 0.73 0.02 mm/s for UTPB and 0.71 ± 0.02 mm/s for CTPB. A slightly lower burning rate for CTPB than that of UTPB reflects that the CTPB sample showed better fire retardancy property than UTPB ones. This is probably ascribed to the enhanced compatibility of TPB with the aids of E-GMA copolymer.
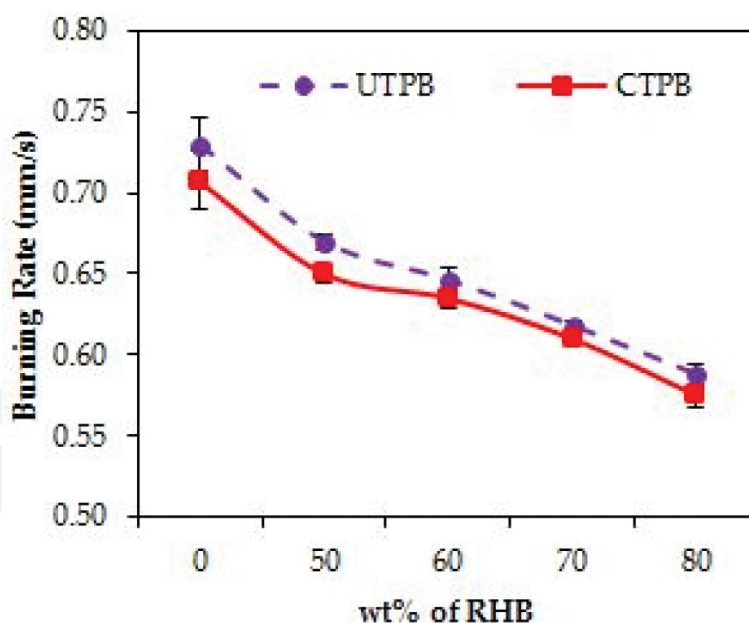

Figure 13. Burning rate of TPB/RHB biocomposites.

For biocomposites containing RHB, the fire retardancy increased by 6–24 % with increasing content of RHB from 40 wt% to 80 wt%. This enhancement might be due to the nature characteristic of silica (relatively high amount, 15–17 % in the raw rice husk) that delayed the combustion [24]. All the CTPB/RHB biocomposites gave lower burning rate (higher fire retardancy) than UTPB/RHB biocomposites. The burning test results showed that the CTPB

(miscible) seemed to improve the interaction between RHB and TPB matrix more effectively than UTPB (immiscible)- based biocomposites.

3.8. Morphological observation

The morphology of the fracture surfaces for (a) 50 wt% RHB/UTPB, (b) 50 wt% RHB/CTPB, (c) 80 wt% RHB/UTPB and (d) 80 wt% RHB/CTPB biocomposites is illustrated in **Figure 14**. Two striking observations can be seen in the surface morphology changes of biocomposites with different RHB contents and TPB matrix types. First, by comparing the effect of RHB contents, the 50 wt% RHB as in **Figure 14(a/b)** was perfectly attached and strongly adhered to the TPB matrix, in which this observation indicates the efficiency of composite material compounding and good fibres-matrix interfacial bonding.
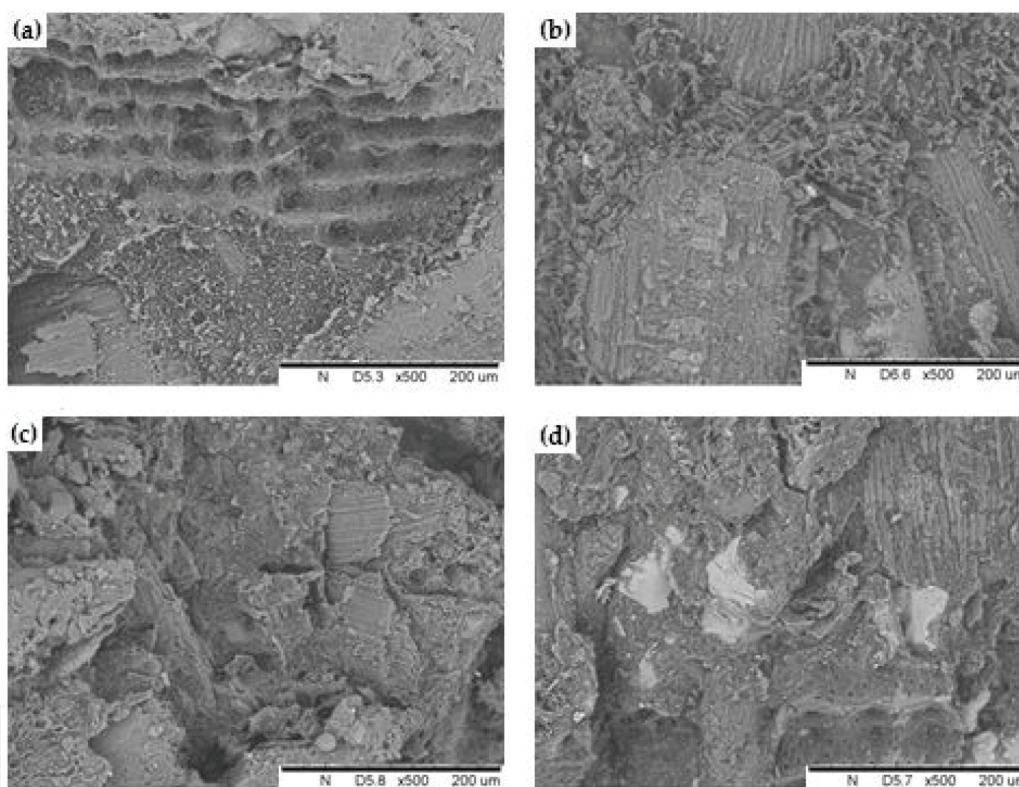

Figure 14. SEM micrograph of (a) 50 wt% RHB/UTPB, (b) 50 wt% RHB/CTPB, (c) 80 wt% RHB/UTPB and (d) 80 wt% RHB/CTPB biocomposites (magnification, 500×).

Meanwhile, the 80 wt% RHB as in **Figure 14(c/d)** showed poorer fibre dispersion and the existence of more clear holes or cavities in the fracture surface morphologies which resulted from insufficient adhesion between filler and matrix. This was then led to the fibre-fibre contact (fibre agglomeration) dominated in the composites. Second, by comparing the effect of TPB matrix types, the UTPB-based biocomposites (**Figure 14(a/c)**) present relatively coarse and obvious phase separation morphology with inhomogeneous filler distribution in the matrix. This can be explained by the fact of the great difference in the polymer solubility parameters

[25], in which rHDPE is nonpolar and rPET is polar. The CTPB-based biocomposites in **Figure 14(b/d)** displayed more homogenous and finer morphology structure which proved the enhanced interfacial adhesion between polymers as well as between fibres and TPB matrix via incorporation of compatibilizer in the matrix.

4. Biocomposite product developments

The authors have carried out the collaboration with Bio Composite Extrusions Sdn. Bhd. and Integral Wood Sdn. Bhd. under TechnoFund grant which produced some of the composite panels and prototypes as shown in **Figure 15** (http://bcextrusions.com/).

Figure 15. Photograph of biocomposite products, buildings and constructions.

5. Conclusion

Rice husk biofibre (RHB)-reinforced recycled high-density polyethylene/recycled polyethylene terephthalate (rHDPE/rPET) biocomposites were fabricated via a two-step melt-blending method. The TPB matrix types (UTPB and CTPB) and RHB contents have significantly affected

the physical properties, mechanical behaviours, thermal stability and morphological performance of biocomposites. As RHB contents increased from 40 to 80 wt%, tensile and flexural properties as well as thermal stability improved remarkably but reduced the impact strength. In the long-term water immersion test, the water absorption and thickness swelling increased with the content of RHB and immersion time regardless of the matrix types. The diffusion coefficient and swelling rate parameter that are determined from the Fickian and swelling model, respectively, increased with the RHB contents. Biocomposites based on CTPB matrix possessed higher mechanical properties and dimensional stability than those based on UTPB matrix. Based on the findings in this study, it is proven that natural fibres/recycled thermoplastic blend biocomposites are suitable for the outdoor applications such as in the field of buildings and constructions.

Acknowledgements

Author details

Ruey Shan Chen[*] and Sahrim Ahmad

*Address all correspondence to: rueyshanchen@hotmail.com

School of Applied Physics, Faculty of Science and Technology, National University of Malaysia, Bangi, Selangor, Malaysia

References

[1] Panthapulakkal S, Sain M. Studies on the water absorption properties of short hemp-glass fiber hybrid polypropylene composites. Journal of Composite Materials. 2007;41:1871–83. DOI:10.1177/0021998307069900

[2] Adhikary KB, Pang S, Staiger MP. Long-term absorption and thickness swelling behaviour of recycled thermoplastics reinforced with *Pinus radiata* sawdust. Chemical Engineering Journal. 2008;142:190–8. DOI:10.1016/j.cej.2007.11.024

[3] Nosbi N, Akil HM, Mohd Ishak ZA, Abu Bakar A. Degradation of compressive properties of pultruded kenaf fiber reinforced composites after immersion in various solutions. Materials and Design. 2010;31(10):4960–4. DOI:10.1016/j.matdes.2010.04.037

[4] Shinoj S, Panigrahi S, Visvanathan R. Water absorption pattern and dimensional stability of oil palm fiber-linear low density polyethylene composites. Journal of Applied Polymer Science. 2010;117(2):1064–75. DOI:10.1002/app.31765

[5] Ping ZH, Nguyen QT, Chen SM, Zhou JQ, Ding YD. States of water in different hydrophilic polymers—DSC and FTIR studies. Polymer. 2001;42:8461–7. doi:10.1016/ S0032-3861(01)00358-5

[6] Scida D, Assarar M, Poilâne C, Ayad R. Influence of hygrothermal ageing on the damage mechanisms of flax-fibre reinforced epoxy composite. Composites Part B: Engineering. 2013;48:51–8. DOI:10.1016/j.compositesb.2012.12.010

[7] Shen CH, Springer GS. Moisture absorption and desorption of composite materials. Journal of Composite Materials. 1976;10:2–20. doi: 10.1177/002199837601000101

[8] Fávaro SL, Lopes MS, De Carvalho Neto AGV, De Santana RR, Radovanovic E. Chemical, morphological, and mechanical analysis of rice husk post-consumer polyethylene composites. Composites: Part A. 2010;41:154–60. DOI:10.1016/j.composi-tesa.2009.09.021

[9] Shi SQ, Gardner DJ. Hygroscopic thickness swelling rate of compression molded wood fiberboard and wood fiber/polymer composites. Composites Part A: Applied Science and Manufacturing. 2006;37(9):1276–85. doi:10.1016/j.compositesa.2005.08.015

[10] Osman EA, Vakhguelt A. Kenaf/recycled jute natural fibers unsaturated polyester composites: water absorption/dimensional stability and mechanical properties. International Journal of Computational Materials Science and Engineering. 2012;1(1): 17 pages. DOI:10.1142/S2047684112500108

[11] Lei Y, Wu Q. Wood plastic composites based on microfibrillar blends of high density polyethylene/poly(ethylene terephthalate). Bioresource Technology. 2010;101:3665–71. DOI:10.1016/j.biortech.2009.12.069

[12] El-Shekeil YA, Sapuan SM, Abdan K, Zainudin E.S. Influence of fiber content on the mechanical and thermal properties of kenaf fiber reinforced thermoplastic polyur-ethane composites. Materials and Design. 2012;40:299–303. DOI:10.1016/j.matdes. 2012.04.003

[13] Ashori A, Nourbakhsh A. Mechanical behavior of agro-residue-reinforced polypropy-lene composites. Journal of Applied Polymer Science. 2009;111:2616–20. DOI:10.1002/ app.29345

[14] Mbarek S, Jaziri M, Chalamet Y, Carrot C. Effect of the viscosity ratio on the morphology and properties of PET/HDPE blends with and without compatibilization. Journal of Applied Polymer Science. 2010;117:1683–94. DOI:10.1002/app.32050

[15] Nourbakhsh A, Baghlani FF, Ashori A. Nano-SiO_2 filled rice husk/polypropylene composites: physico-mechanical properties. Industrial Crops and Products. 2011;33:183–7. DOI:10.1016/j.indcrop.2010.10.010

[16]   Yang W, Hu Y, Tai Q, Lu H, Song L, Yuen RKK. Fire and mechanical performance of nanoclay reinforced glass-fiber/PBT composites containing aluminium hypophosphite particles. Manufacturing. 2011;42(7):794–800. DOI:10.1016/j.compositesa.2011.03.009

[17]   Kiziltas A, Gardner D, Han Y, Yang, H-S. Thermal properties of microcrystalline cellulose-filled PET–PTT blend polymer composites. Journal of Thermal Analysis and Calorimetry. 2011;103:163–70. DOI:10.1007/s10973-010-0894-6

[18]   Yao F, Wu Q, Lei Y, Xu Y. Rice straw fiber-reinforced high-density polyethylene composite: effect of fiber type and loading. Industrial Crops and Products. 2008;28(1): 63–72. DOI:10.1016/j.indcrop.2008.01.007

[19]   Chun KS, Husseinsyah S, Syazwani NF. Properties of kapok husk-filled linear low-density polyethylene ecocomposites: effect of polyethylene-grafted acrylic acid. Journal of Thermoplastic Composite Materials. 2015. DOI:10.1177/0892705715583175

[20]   Kim H-S, Lee B-H, Choi S-W, Kim S, Kim H-J. The effect of types of maleic anhydride-grafted polypropylene (MAPP) on the interfacial adhesion properties of bio-flour-filled polypropylene composites. Composites: Part A. 2007;38:1473–82. DOI:10.1016/j.compositesa.2007.01.004

[21]   Khalil R, Chryss A, Jollands M, Bhattacharya S. Effect of coupling agents on the crystallinity and viscoelastic properties of composites of rice hull ash-filled polypropylene. Journal of Materials Science. 2007;42(24):10219–27. DOI:10.1007/s10853-007-1732-5

[22]   Kim H-S, Kim S, Kim H-J, Yang H-S. Thermal properties of bio-flour-filled polyolefin composites with different compatibilizing agent type and content. Thermochimica Acta. 2006;451(1–2):181–8. DOI:10.1016/j.tca.2006.09.013

[23]   Deka BK, Maji TK. Study on the properties of nanocomposite based on high density polyethylene, polypropylene, polyvinyl chloride and wood. Composites Part A: Applied Science and Manufacturing. 2011;42(6):686–93. DOI:10.1016/j.compositesa.2011.02.009

[24]   Arora S, Kumar M, Kumar M. Flammability and thermal degradation studies of PVA/rice husk composites. Journal of Reinforced Plastics and Composites. 2012;31(2):85–93. DOI:10.1177/0731684411431765

[25]   Chen RS, Ab Ghani MH, Salleh MN, Ahmad S, Gan S. Influence of blend composition and compatibilizer on mechanical and morphological properties of recycled HDPE/PET blends. Materials Sciences and Application. 2014;5(13):943–52. DOI:10.4236/msa.2014.513096